Organic Process Research & Development **2006**, *10,* 203–211

Polymorph and Particle Size Control of PPAR Compounds PF00287586 and AG035029

Billie J. Kline,* James Saenz, Nebojša Stanković, and Mark B. Mitchell

Chemical Research and Development, Pfizer, Inc., 10578 Science Center Drive, San Diego, California 92121, U.S.A.

Abstract:

Development of polymorph control procedures for PF00287586 and AG035029 is described herein. For PF00287586, investigations were undertaken to control formation of both identified polymorphs, Form A and Form B. Solvent screening methodology was employed to find a solvent system that inhibited the solvent-mediated transformation of A to B so that the thermodynamically less stable Form A could be generated. For Form B, meta-stable zone width (MSZW) determination was performed and used to devise a controlled crystallization protocol to furnish Form B with improved flow and physical characteristics. For AG035029, both seeded crystallization and solvent-mediated transformation methods to generate Form B were investigated. During the development of the seeded crystallization, challenges arose when a ring of spontaneously nucleated Form A would form above the liquid level in the vessel during the cooling phase. Extraneous seeding from this "beard" invariably resulted in crystallization of Form A. A solution was developed by modification of the solvent system. Finally, optimization of the solvent-mediated transformation is presented.

Introduction

PF00287586 and AG035029 are peroxisome proliferator-activated receptor (PPAR) inhibitors for the treatment of diabetes. Whilst they are both structurally related carboxylic acids possessing crystal lattices rich in hydrogen bonds, they actually differ significantly in polymorphic behavior (Table 1). For PF00287586, the overall objective of the work was to formulate reliable procedures to prepare both Forms A and B and to manipulate the particle size distribution of Form B such that larger particles were generated using a seeded crystallization strategy. For AG035029, the goal was to prepare Form B, using either seeded cooling crystallization or solvent-mediated transformation.

In performing this work, a toolbox of technologies was utilized so that screening and accurate control of process variables could be achieved. A combination of automated lab reactors (ALRs), in situ analytic probes, and screening matrixes were essential so that the peculiarities presented in the various situations could be approached more rationally. These technologies expedited process development such that up-scaling to deliver the first batch of large-scale quantities of active pharmaceutical ingredient (API) could be accomplished in an accelerated time frame.

* To whom correspondence should be addressed. E-mail: billie.kline@pfizer.com.

Table 1. **Properties of PF00287586 and AG035029**

property	PF00287586	AG035029
polymorphic behavior	monotropic	enantiotropic
transition temperature	N/A	~95 °C
Form A melting point	72 °C	173 °C
Form B melting point	106 °C	164 °C
stable form at rt	Form B	Form B

Results and Discussion

PF00287586 Crystallization. Early crystallizations of PF00287586 from ethyl acetate/*n*-heptane furnished Form A, the only known form at that stage. Form B appeared

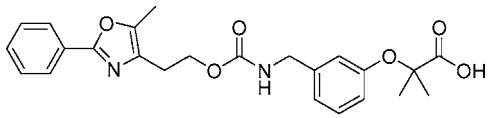

PF00287586

serendipitously during subsequent up-scaling of this procedure. Interestingly, once Form B was generated, the preparation of Form A could not be repeated, suggesting that Form A is an example of a "disappearing polymorph".[1] Research was directed toward developing a new protocol for preparation of Form A.

To have any chance of developing a crystallization procedure for the thermodynamically less stable polymorph (Form A), it was essential to find a solvent system in which the rate of A→B solvent-mediated transformation was negligible. To this end, a screen was conducted utilizing the Zinsser SOPHAS platform to dispense 20 mg of Form A to each position of a 96 well-plate followed by 100 μL of solvent. The solvent composition in each well was varied in accord with the matrix depicted in Figure 1.

The plate was briefly agitated and allowed to stand at ambient temperature overnight. The plate was then visually examined for solids, and where present, the respective well was analyzed by Raman spectroscopy. Form B could be readily distinguished from Form A by the presence of a strong scatter at 1075 cm^{-1} and a single scatter at 1350 cm^{-1}. Form A itself lacked the 1075 cm^{-1} scatter and possessed a "double" scatter centered at 1350 cm^{-1} (Figure 2a). The quotient for the intensity of the 1075 cm^{-1} band versus that of a constant band at 1603 cm^{-1} was plotted against sample number to aid in identification of samples that had not transformed to Form B. Such samples would be expected to have a low quotient value, and this indeed is where hits were observed (Figure 2b).

(1) Dunitz, J. D.; Bernstein, J. *Acc. Chem. Res.* **1995**, *28*, 193−200.

10.1021/op050176r CCC: $33.50
Published on Web 03/02/2006

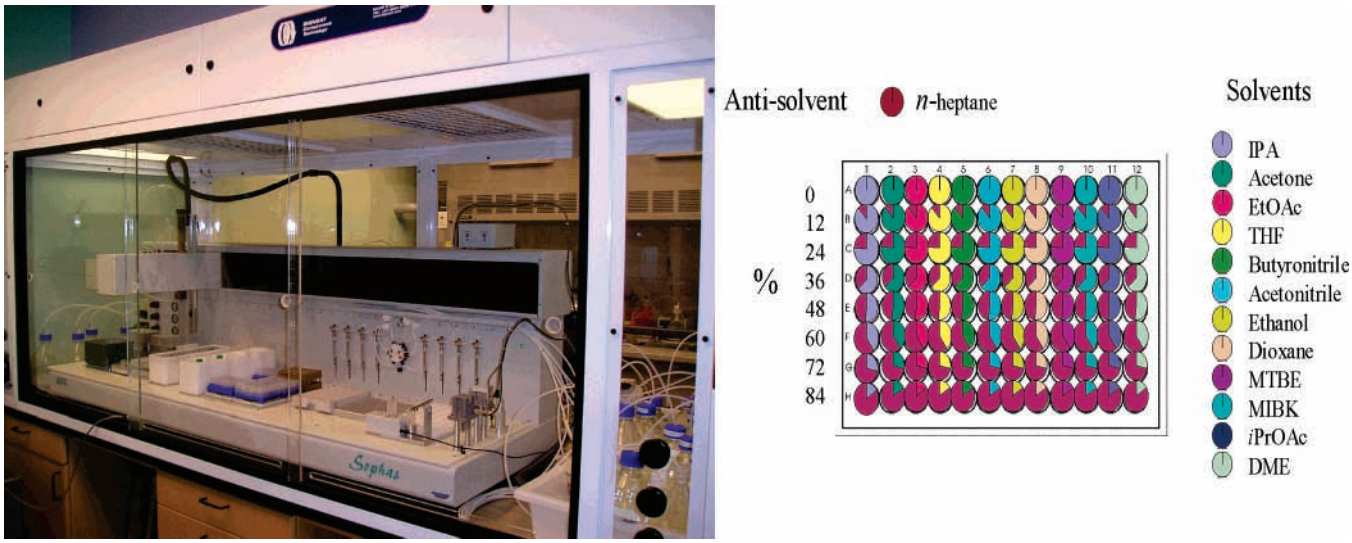

Figure 1. **Solvent screening matrix dispensed using Zinsser SOPHAS.**

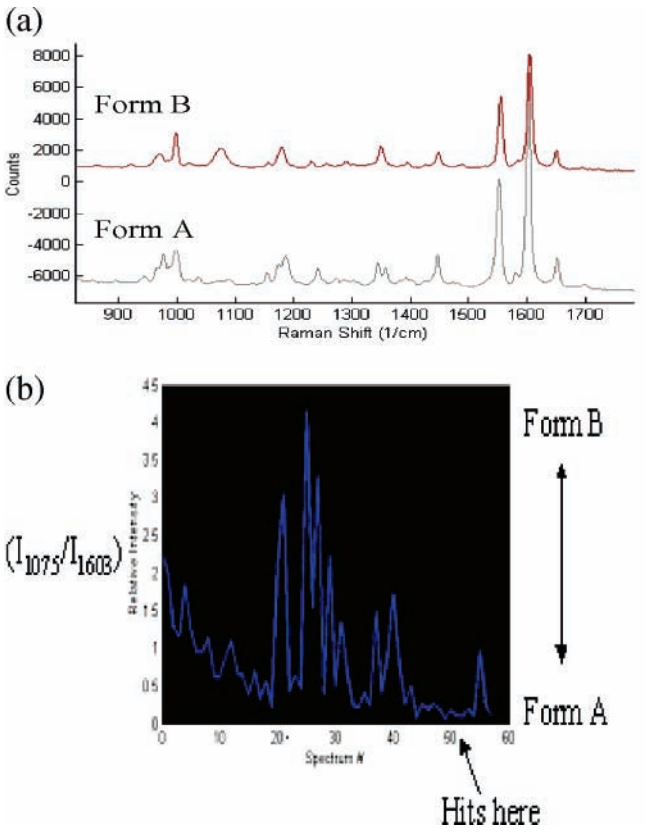

Figure 2. **(a) Raman spectra for Form A and Form B. (b) Plot of intensity quotient for the 1075 cm^{-1} band of the Raman spectra over the 1603 cm^{-1} band for each well number.**

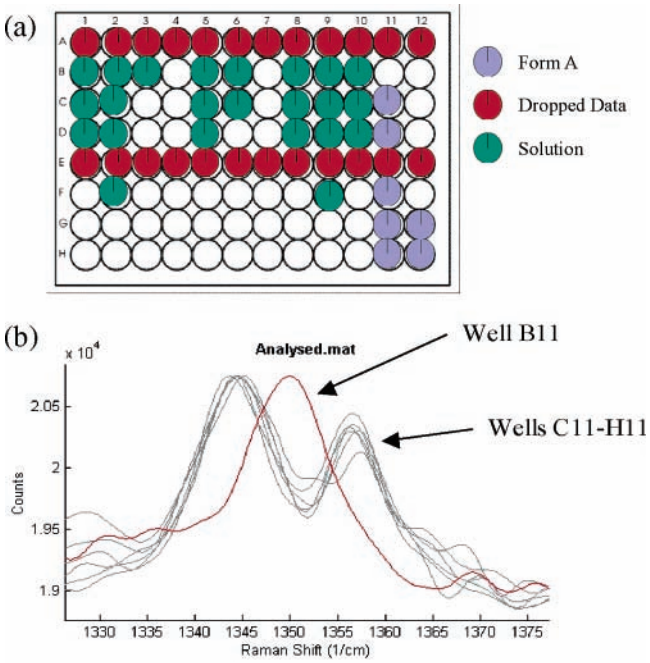

Figure 3. **(a) Hits indicating Form A formation via Raman analysis. (b) Raman spectra at 1350 cm^{-1} band signifying shift from generation of Form B in well B11 to that of Form A in downstream wells with increasing anti-solvent in *i*PrOAc.**

Two solvent systems were identified in which solvent-mediated transformation was inhibited, *i*-PrOAc/*n*-heptane (>24% *n*-heptane) and DME/*n*-heptane (>72% *n*-heptane) (Figure 3). The trend of inhibited solvent-mediated transformation relative to increasing anti-solvent content is in accordance with the work of Grant.[2] Note also the marked behavior change in the swap from EtOAc (facile solvent-mediated transformation) to *i*-PrOAc. Whilst these solvents may outwardly appear to be quite similar, a principal component analysis (PCA) performed in-house clustering 108 different solvents based upon 15 physical parameters indicates that they actually fall in markedly different areas of PCA space.[3] In consequence they are anticipated to be less similar than initially expected. The *i*-PrOAc/*n*-heptane mixture is a preferred process solvent system and was selected over DME/*n*-heptane as it has the additional advantage of volume efficiency—less anti-solvent could be tolerated in the former case. A 62:38 ratio of *i*-PrOAc/*n*-heptane was chosen for subsequent meta-stable zone width (MSZW) studies. It was essential to get a handle on the meta-

(2) Gu, C.-H.; Young, V., Jr.; Grant, D. J. W. *J. Pharm. Sci.* **2001**, *90*, 1878−1889.

(3) Carlson, R.; Lundstedt, T.; Albano, C. *Acta Chem. Scand., B: Org. Chem. Biochem.* **1985**, *B39*, 79−91.

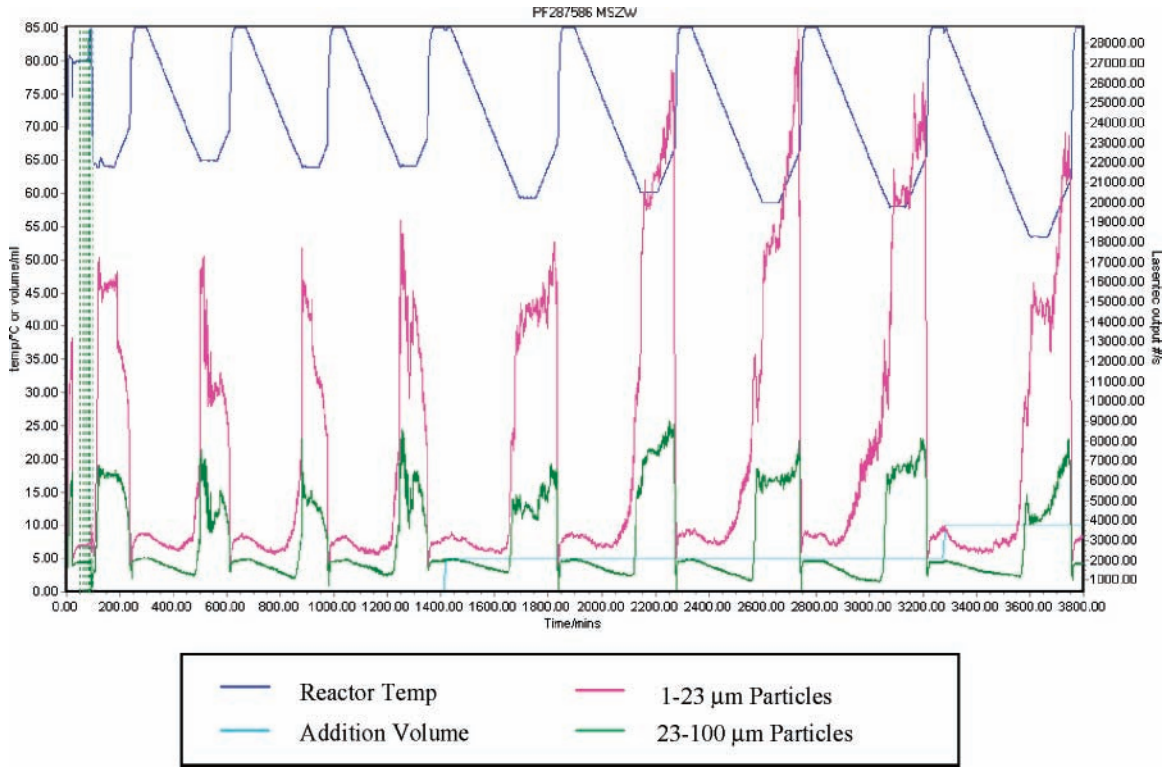

Figure 4. **MSZW determination using AutoMate and FBRM.**

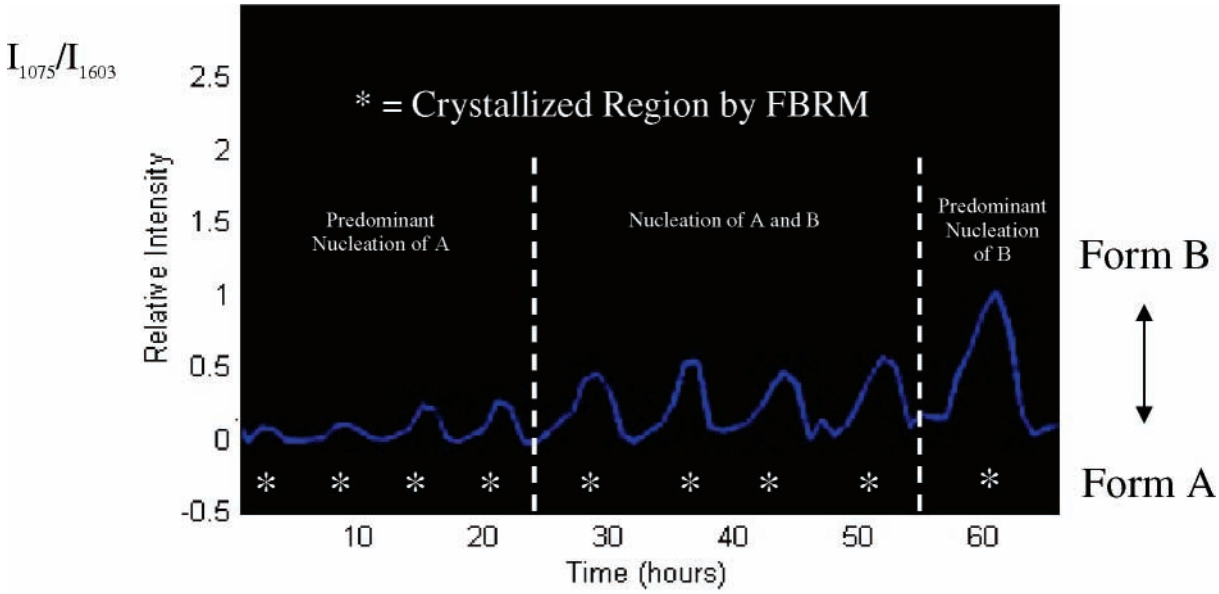

Figure 5. **Raman measurements during MSZW determination.**

stable zone since this provides the only "window of opportunity" for efficacious seeding.

The MSZW was determined using a 50-mL HEL AutoMate reactor linked to a Lasentec focused beam reflectance measurement (FBRM) S400Q probe. A ramp rate of 0.1 °C/min was employed for the heating and cooling cycles, utilizing a 1−23 μm range for evaluation of cloud point, and 23−100 μm range for the dissolution point at several dilutions (Figure 4). Raman spectra were also recorded concurrently using the Kaiser RXN1 instrument (Figure 5).

The Raman data indicated that at the highest concentration, nucleation of Form A was predominant with an increasing tendency for nucleation of Form B at higher dilutions. FBRM also revealed that once mixed nucleation occurred the transformation of A→B became relatively facile as signaled by the dissolution shoulder in the FBRM. The data were consistent with a solubility profile that qualitatively looks like that depicted in Figure 6a. Cooling a fairly concentrated solution results in crossing the meta-stable limit for Form A first, resulting in nucleation of this form. As dilution is increased, the meta-stable limits for Form A and Form B are similar, and hence mixed nucleation is anticipated. As dilution is increased further, the meta-stable limit for Form B is crossed first, and hence predominant nucleation

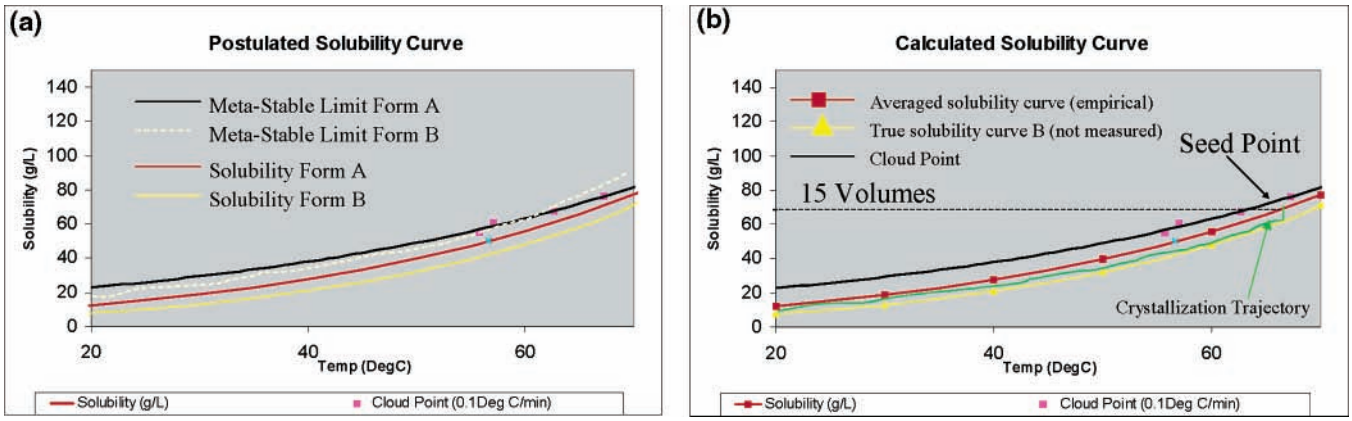

Figure 6. **(a) Proposed solubility profile (qualitative). (b) Averaged solubility data for Form A/B.**

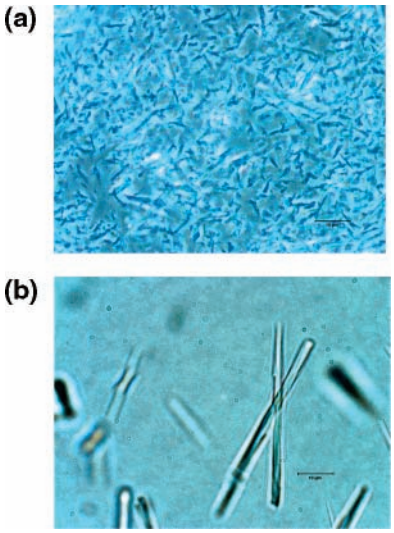

Figure 7. **Optical microscopy: (a) Uncontrolled crystallization. (b) Controlled crystallization. Scale for (a) and (b): 10 μm.**

of this form is expected. Sufficient data had now been collected to devise a controlled crystallization experiment; however, this was not performed due to the decision of the project team to up-scale the Form B protocol.

The more thermodynamically stable Form B had been previously prepared by crystallization from ethyl acetate/*n*-heptane, affording a solid with poor bulk properties. In particular the material was found to be very slow to filter, ultimately furnishing a dried powder that was very electrostatic and difficult to handle. This was symptomatic of particle size distribution comprising a large fines count, which was confirmed by optical microscopy (Figure 7a).

To improve the situation, a controlled crystallization procedure was devised utilizing *i*-PrOAc/*n*-heptane as solvent to take advantage of the solubility data already collected (Figure 6b). Note that the empirical dissolution points were fitted to the van't Hoff expression, furnishing an averaged solubility curve for Form A/B. The key objective was to seed in the meta-stable zone, and this averaged value would work well for this purpose (since the true value for Form B must, by definition, by less than the averaged value). It was convenient to work at 15 volumes of solvent, giving rise to the following crystallization regime:

- Heat to 80 °C to furnish clear solution
- Rapidly cool to 70 °C
- Cool at 0.5 °C/min to 65 °C
- Seed at 65 °C (1 wt % seed)
- Isothermal hold for 1 h
- Cool at 0.1 °C/min to 20 °C

Initial evaluation at 50-mL scale utilizing Mettler Multimax and FBRM indicated that agglomeration of seeds occurred during the isothermal hold post seeding (Figure 8a). The slow cooling rate was employed after the isothermal hold to ensure that secondary contact nucleation and growth were faster than the cooling rate. Otherwise, the cloud point would be crossed, and spontaneous nucleation would occur, generating many fines. The isolated solid was readily filtered and had a much larger particle size (Figure 7b). The post seeding agglomeration only occurred when using the fine electrostatic material as seed stock; when the larger needles were employed, this unsurprisingly did not occur.

The process was validated at 2-L scale with HEL SIMULAR and FBRM, furnishing a readily filtered, non-electrostatic solid with comparable crystal size distribution (CSD) to the 50-mL evaluation batches (Figure 8b). The process was transferred to the material production group (MPG) whence 1.5 kg of Form B was successfully prepared without incident.

AG035029 Crystallization. AG035029 exists as two different forms, Form A (mp 173 °C) and Form B (mp 164 °C). The polymorphic relationship is enantiotropic, with a

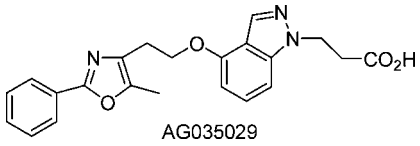

AG035029

transition temperature of approximately 95 °C. Thus, the lower-melting form (Form B) is more stable at room temperature, whilst Form A nucleates first in agreement with Ostwald's rule of stages. Initial attempts at seeding with Form B proved to be capricious, oftentimes resulting in crystallization of Form A, despite the apparent persistence of Form B seeds. As with PF00287586, a systemized approach to the problem was adopted. The MSZW was determined using HEL AutoMate and Lasentec FBRM. Initial experiments

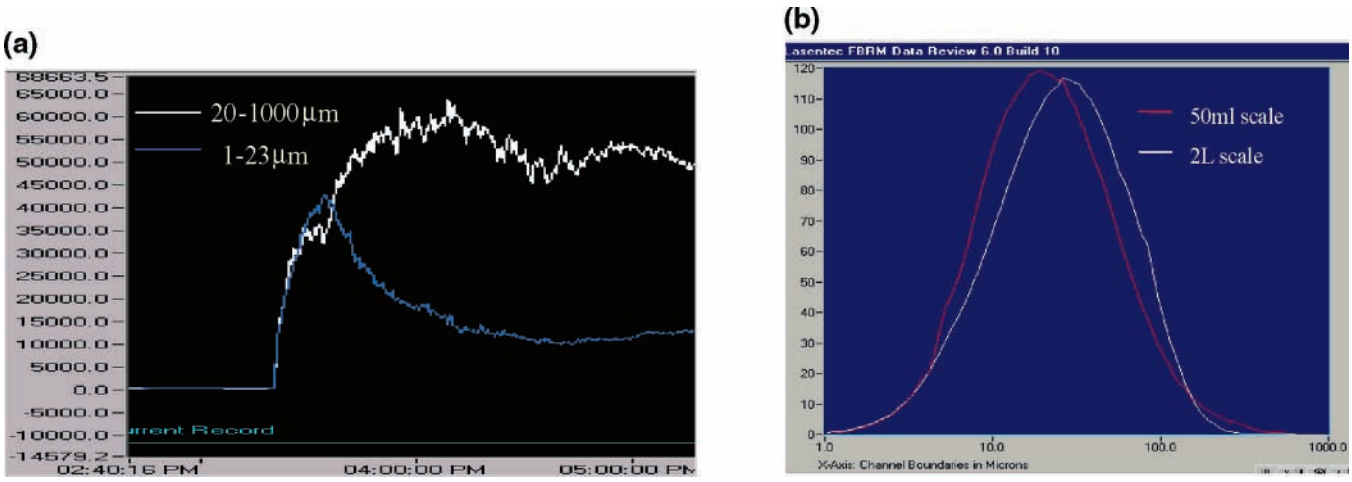

Figure 8. **FBRM data: (a) Post-seed agglomeration. (b) CSD comparison.**

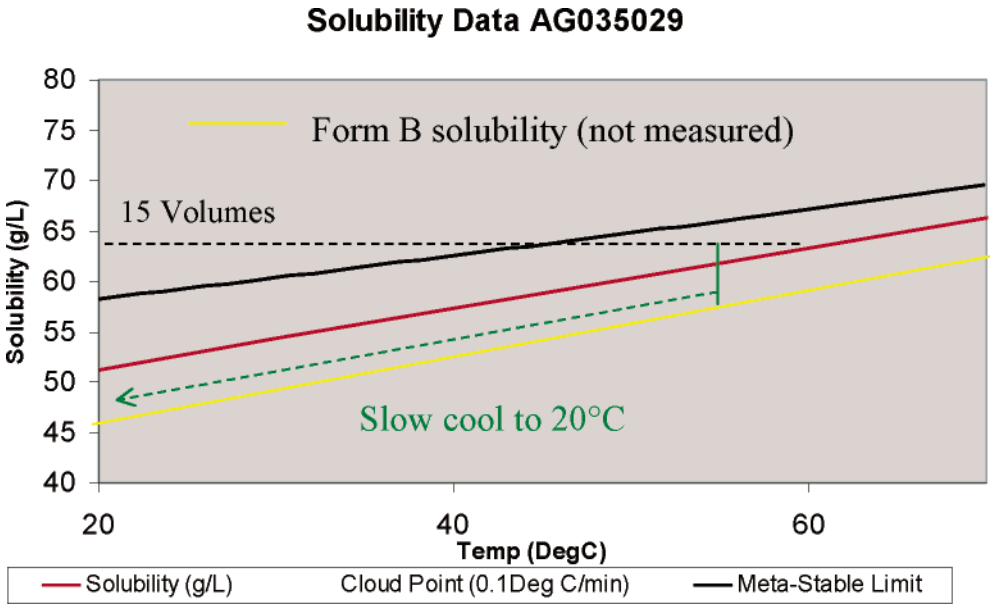

Figure 9. **Solubility profile for AG035029.**

employed neat DME as solvent; however, crystallization characteristics were poor from this system. Use of 85:15 DME/*n*-heptane greatly improved the situation, and the solubility curve is depicted in Figure 9. This clearly indicates a very wide MSZW of approximately 30 °C.

The initial crystallization protocol involved heating of AG035029 in 15 volumes of 85:15 DME/*n*-heptane to 80 °C to furnish a clear solution. After rapid cooling to 60 °C, the cooling rate was then slowed to 0.5 °C/min until reaching 55 °C; the solution was then seeded with 1 wt % of Form B. After an isothermal hold for 60 min, the mixture was cooled at 0.1 °C/min to 20 °C. The crystallization procedure was tested at the 50-mL scale using the toxicological batch of AG035029 and progressed as expected furnishing Form B (as determined by Raman spectroscopy, Figure 10). However, a subsequent experiment resulted in spontaneous nucleation prior to seed addition, leading to formation of Form A (Figure 11).

The apparent reduction in MSZW was traced to fouling of the reactor wall ("bearding") by AG035029. This spontaneously nucleated "beard" was Form A (Ostwald's rule of stages), and the spurious contamination of the batch by this material resulted in bulk crystallization of Form A. The beard fouled the batch in one of two ways: by seeding the batch prior to the intentional Form B seeding as shown in Figure 11a or by overriding the Form B seeding. This latter case was observed by FBRM as a secondary seeded nucleation event (Figure 12).

The fouling of the glass wall stems from strong adhesive forces between the glass surface and AG035029. While adhesion of material to a glass surface can be attributed to several factors including surface roughness and contact angle, hydrogen bonding, or van der Waals interactions, the most likely candidate in this case was thought to be hydrogen bonding, as the chemical structure is rich in this component. To overcome the adhesion between the carboxylic acid and the hydrophilic glass surface, a high-boiling solvent was required that could provide an alternate source of hydrogen bonding, such as a longer-chain alcohol. The former requirement would ensure the liquid composition at the meniscus would be rich in the alcohol component and essentially trap the API in the solvent mixture. Figure 13 shows snapshots

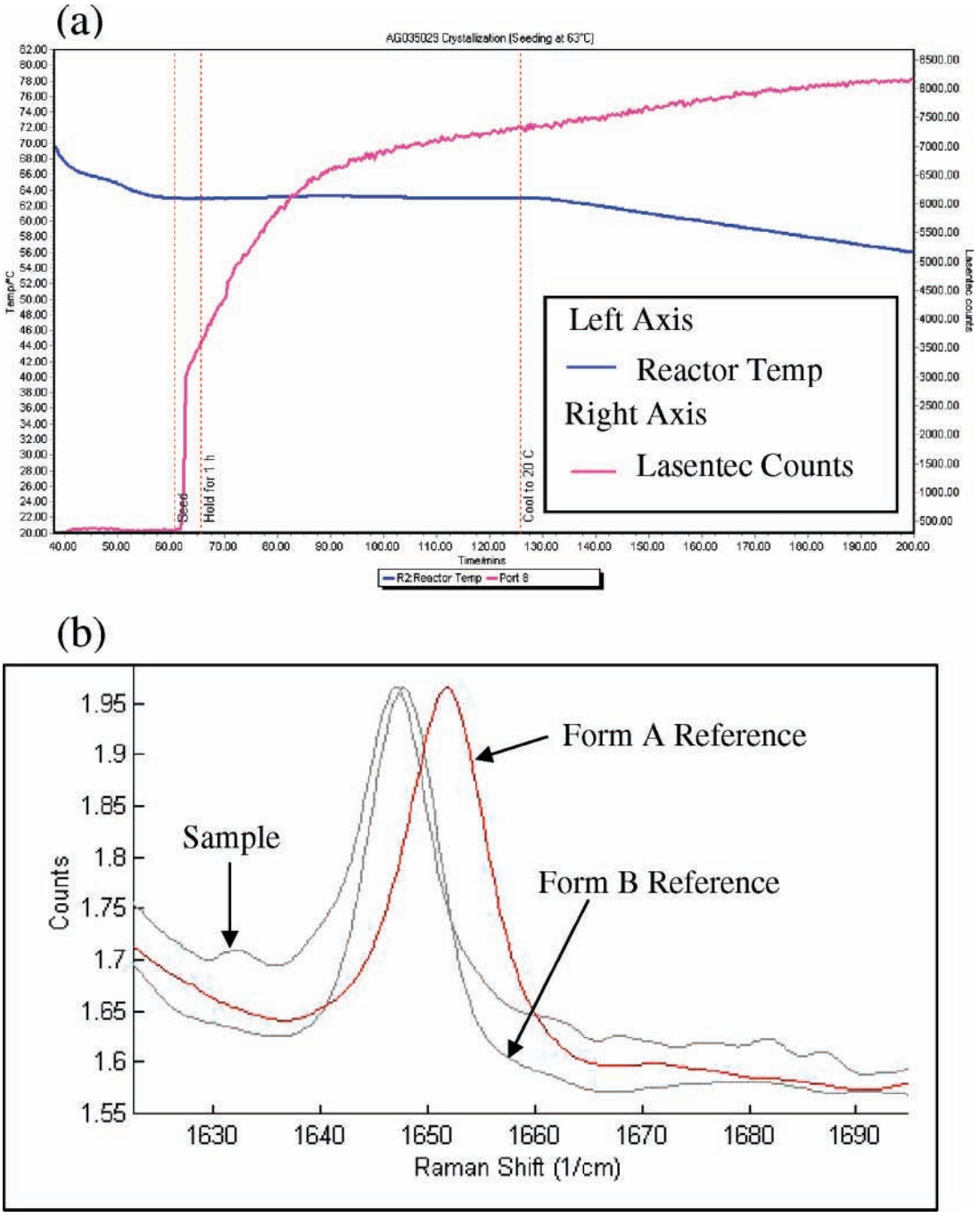

Figure 10. **(a) Crystallization profile for successful seeding, resulting in the generation of Form B. (b) Raman spectra of carbonyl region, indicating that the sample spectra corresponds to the Form B reference.**

of the reactor wall with and without the addition of *n*-butanol. In the top row, the fouling progresses until the entire surface above the liquid is covered in Form A that spontaneously nucleated whereas in the bottom row, the area above the level of the liquid is clear throughout the entire experiment. Accordingly, 9 vol % of *n*-butanol was added to the reaction mixture, and this successfully eliminated the bearding effect.

Whilst the addition of *n*-butanol afforded a solution to the fouling problem and Form B could be generated when employing the toxicological batch, use of AG035029 of lower purity still resulted in the crystallization of Form A. FBRM studies clearly indicated that this was the result of nucleation inhibition by the main diacid impurity, present at 1% levels (Figure 14).

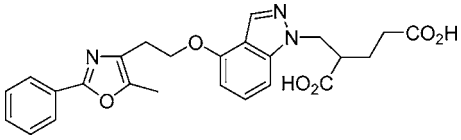

Having identified these factors, the process could now be reliably reproduced. The key factors to establish process control and guarantee generation of Form B were:

- use of *n*-butanol as a cosolvent

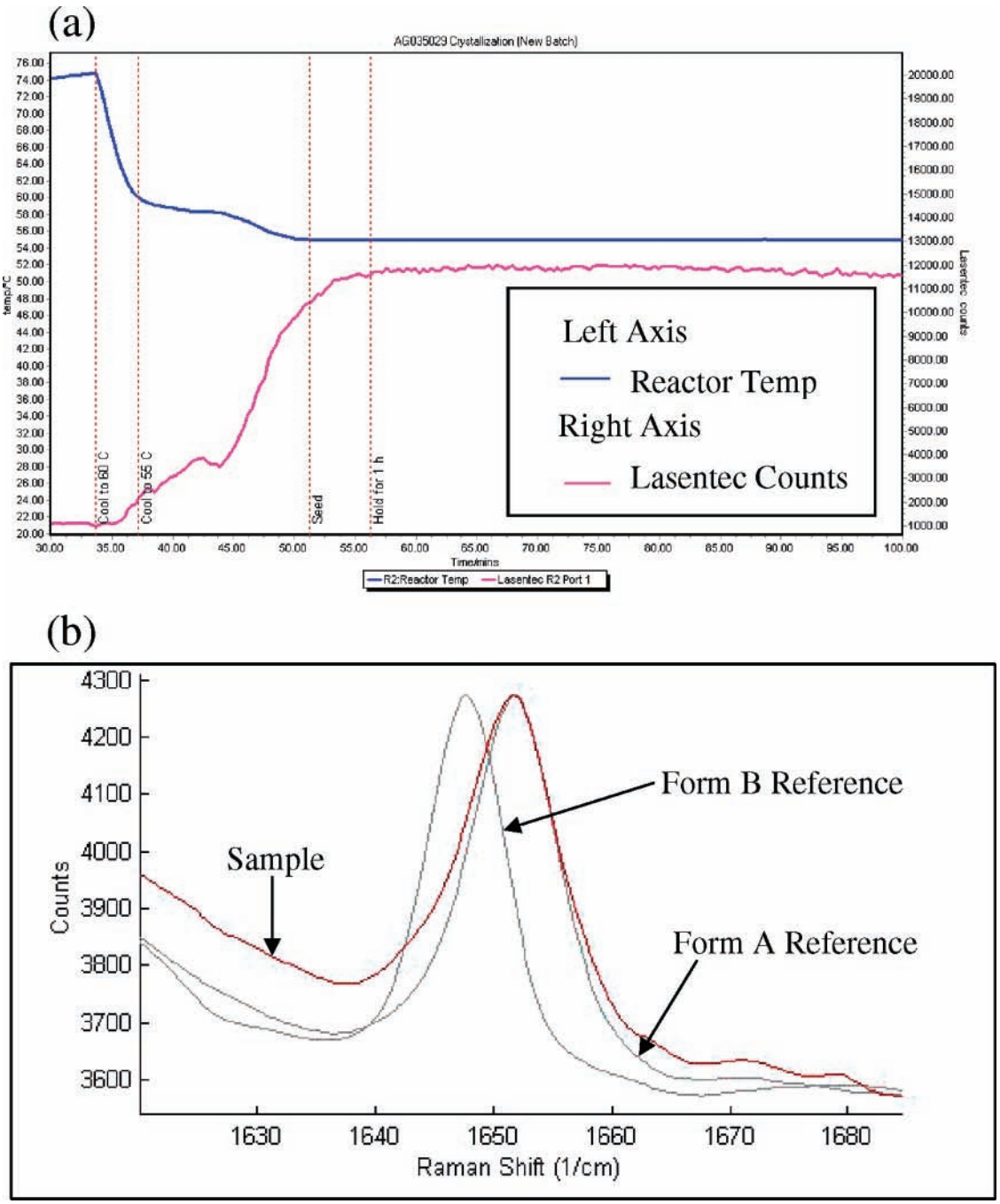

Figure 11. **(a) Crystallization profile for unsuccessful seeding, resulting in generation of Form A. (b) Raman spectra of carbonyl region, indicating that the sample spectrum corresponds to the Form A reference.**

- use of AG035029 Form A with a purity of ≥99.8%
- seeding in the meta-stable zone with controlled cooling

Polymorph control was subsequently demonstrated at 470-g scale with toxicological lot material, using a 20-L QVF reactor with Huber thermostat control (in association with the Materials Production Group). Form B was successfully isolated in 74% yield as a readily filtered solid.

AG035029 Solvent-Mediated Polymorph Transformation (SMPT). The mechanics of SMPT center around the conversion of a stirred slurry to a slurry of a more thermodynamically stable crystal form, exploiting the fact that a saturated solution of the meta-stable modification is by definition supersaturated in the stable one.[2] Since the transformation rate in different solvents varies a great deal, it is essential to identify a solvent that has favorable process kinetics.

To reach this goal, a series of solvent screens were conducted, which provided data on transformation rate and solubility.[4] Eleven different, commonly used solvents were chosen along with one solvent mixture (THF/EtOH). AG035029 Form A was used in 1-g aliquots; each sample was dissolved in 10 volumes of solvent and stirred at room temperature. The system was closed and allowed to stir for 24 h. Subsequently, 1.5 mL of each mixture was filtered and

(4) Experiments were conducted using RS-10 Stem Blocks.

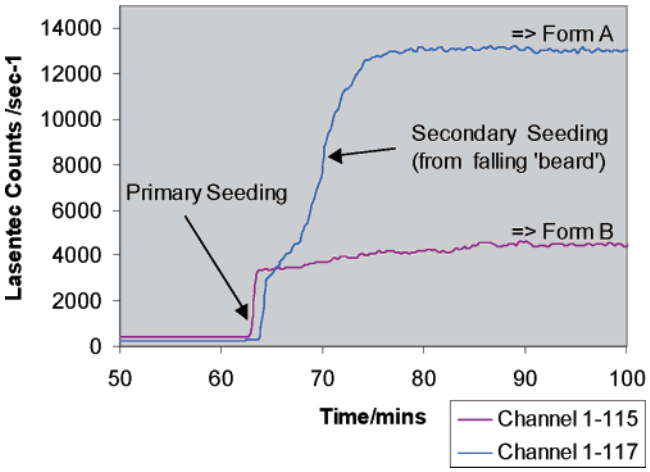

Figure 12. **Lasentec profile during isothermal hold. Example of desired situation to obtain Form B and undesired secondary seeding (from falling "beard").**

Table 2. **Initial solvent screens at room temperature and at 40 °C**

solvent	rt	40 °C	solvent	rt	40 °C
EtOAc	A > B	A = B	MTBE	A = B	A > B
IPA	A	B > A	MIBK	A	A > B
acetone	A > B	B > A	MeOH	A	B
THF	A > B	n/a	ACN	n/a	B
EtOH	A	B	THF/EtOH	A > B	B
dioxane	A	B	TFT	A > B	n/a

dried, providing 100−180 mg of material, depending upon solubility. Each sample was analyzed by Raman spectroscopy to determine polymorphic form. Data from these studies is presented in Table 2.

The initial data indicated that transformation is faster at higher temperatures (predictably). Subsequent studies showed severe degradation of the product at 50 °C over an extended period of time, which implied that 40 °C is the optimal operational temperature. Results obtained from the room-temperature conversion identified solvents that facilitated as well as those that retarded transformation. At room temperature, *tert*-butyl methyl ether showed the fastest rate of transformation, which was only marginally successful since complete conversion was not achieved. At 40 °C, however, transformation rate greatly increased across the board. Moreover, ethanol, methanol, 1,4-dioxane, acetonitrile, and THF/EtOH mixture advanced the transformation to its completion. Since the material recovery from acetonitrile was very low, it was abandoned whilst the other four solvents were further explored.

Table 3. **Solvent screens at 40 °C, 5-gram scale**

solvent	Form (after 24 h at 40 °C)	(after 48 h at 40°C)	(after 144 h at 40 °C)	recovery (%)
EtOHaft	A	A	A≫B	90
THF/EtOH	B	n/a	n/a	57
1,4-dioxane	A≫B	A≫B	B	>20
MeOH	A>B	A	B≫A	94

A second set of experiments focused on this select group of solvents, under the same conditions, but at a larger scale. Previous experiments have shown that a change in scale can have an impact on transformation rate. Each batch contained 5 g of material and was sampled at 24-hour intervals. Table 3 shows the data obtained.

As seen from the table, THF/EtOH provided the best transformation rate, followed by 1,4-dioxane. Material recovered from the THF/EtOH mixture accounted for 57% of the mass balance, which was low but understandable due to good solubility of AG035029 in THF. Material recovery

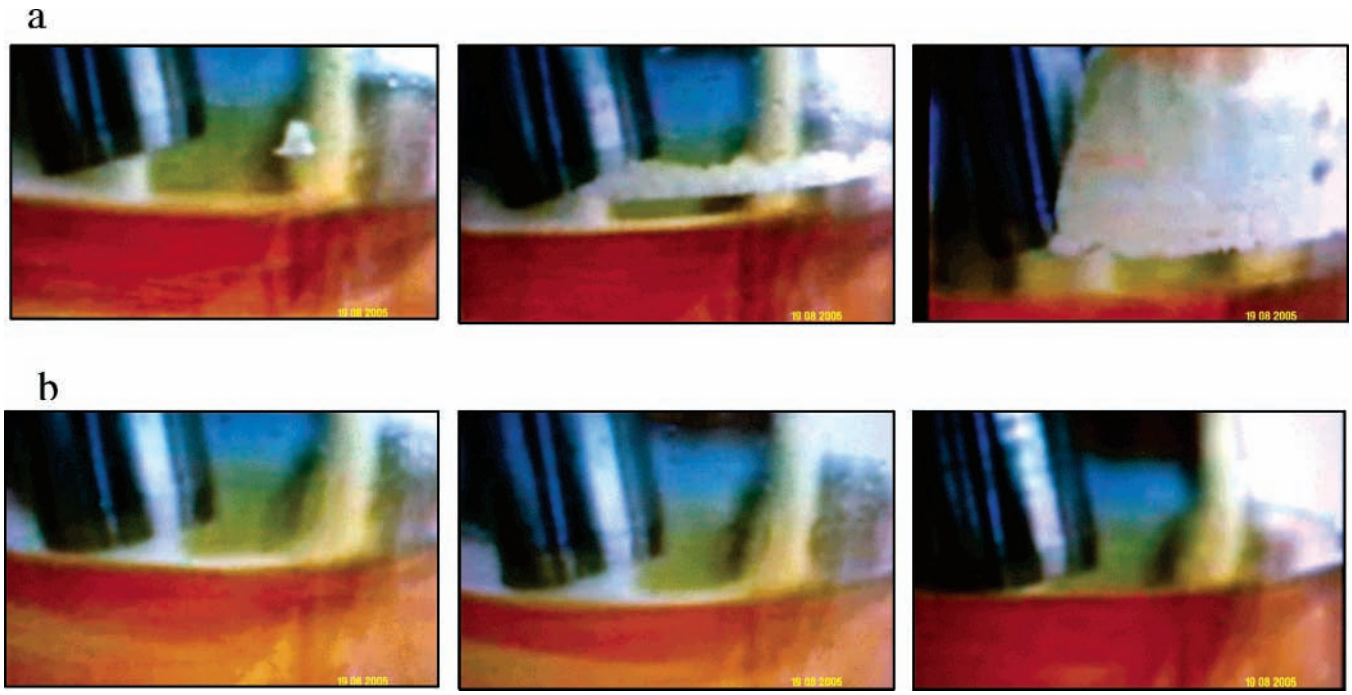

Figure 13. **(a) Snapshots of reaction without *n*-butanol addition at times 0, 5, and 30 min. (b) Snapshots of reaction with *n*-butanol addition at times 0, 5, and 30 min.**

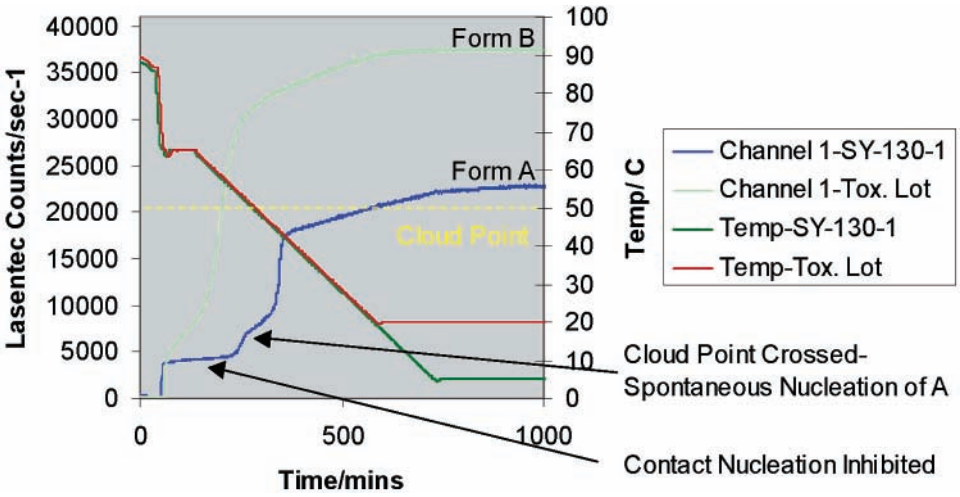

Figure 14. **Nucleation inhibition by diacid impurity and observed by FBRM.**

from 1,4-dioxane was so poor it was abandoned. This experiment also distinguished the alcohols from each other, indicating faster transformation with MeOH. However, it also revealed that on scale, both alcohols would prove valueless since there was a five-day difference in conversion time, when compared to THF/EtOH. Interestingly enough, relatively low solubility of material in both alcohols ensured respectable recovery. These observations led to a proposal that an appropriate mixture of THF and either alcohol would yield a timely transformation with acceptable recovery.

Apart from the solvent, batch size also appeared to greatly influence transformation rate. Whilst keeping variables such as temperature, concentration, and material purity constant, transformation rate inevitably slowed with an increase in scale. The influence of scale has been observed to be dependent on convective mass transfer, i.e., the mechanical contact between the agitator/vessel and the crystals.[5,6] On scale, such contacts are more infrequent, while smaller vessels, using magnetic stirrers, have a much higher frequency of contact. Similar trends were observed during the solvent screens, scaling up from 1 to 5 g, when it took 3−5 days longer for the transformation to be complete.

Conclusion

In the two case studies presented, controlled crystallization and solvent-mediated transformations were successfully developed that reliably addressed the critical problems of polymorphic form and particle size that commonly crop up in the pharmaceutical industry. Development of consistent crystallization methods has been more of an art than science. However, the use of screening methodologies to comprehensively cover solvent space and in situ analytical tools to visually confirm particle formation, measure particle size, and determine polymorphic form provides significant insight towards more rationally designing crystallization processes.

Acknowledgment

We thank Bing Shi for offline optical microscopy, Tim Kennedy and Ming Guo for assistance with MPG operations, and Shu Yu for overall project guidance.

Received for review September 21, 2005.

OP050176R

(5) Ferrari, E. S.; Davey, R. J.; Cross, W. I.; Gillon, A. L.; Towler, C. S. *Cryst. Growth Des.* **2002**, *3*, 53−60.
(6) Davey, R. J.; Blagden, N.; Righini, S.; Alison, H.; Ferrari, E. S. *J. Phys. Chem.* **2002**, *106*, 1954−1959.